

## Study on spectroscopic and quantum chemical calculations of levosimendan

S Bahçeli<sup>a\*</sup> & H Gökce<sup>b</sup>

<sup>a</sup>Süleyman Demirel University, Faculty of Arts and Sciences, Physics Department, East Çünür Campus, 32260, Isparta, Turkey

<sup>b</sup>Vocational High School of Health Services, Giresun University, Güre Campus, 28200, Giresun, Turkey

\*E-mail: semihabahceli@sdu.edu.tr

Received 6 April 2013; revised 29 October 2013; accepted 18 February 2014

In the present study, FT-IR, micro-Raman and UV-Vis. spectra of levosimendan molecule, ( $C_{14}H_{12}N_6O$ ), have been experimentally recorded and the molecular geometry, vibrational frequencies, electronic absorption spectrum, HOMO-LUMO analysis, natural bond orbital (NBO) analysis, molecular electrostatic potential (MEP), thermodynamic properties and atomic charges of title molecule have been calculated by using density functional theory (DFT/B3LYP) method with 6-311++G(d,p) basis set in the ground state. The calculated vibrational results are found to be good agreement with experimental data.

**Keywords:** Levosimendan, FT-IR, Micro-Raman spectra, UV-Vis spectra, DFT method

### 1 Introduction

Over two decades levosimendan has been widely used in the drug industry and medicine. Levosimendan is a novel calcium sensitisier and pharmacological agent for patients with severe heart failure<sup>1-6</sup>. In clinical studies, levosimendan is used to increase the cardiac output and to lower cardiac filling pressures<sup>7</sup>. Recently, levosimendan has been proposed to be superior to standart inotropes and its several promising clinical applications have been arisen<sup>8</sup>. However, the levosimendan molecule is chemically a pyridazinone-dinitrile derivative and some other 6-phenyl 4,5-dihydro-3(2H)-pyridazinone derivatives have been studied by using IR and <sup>1</sup>H NMR spectroscopies<sup>9-11</sup>.

On the other hand, Hartree-Fock (HF), density functional theory (DFT) and Moller-Plesset perturbation theory called ab-initio methods can be based on the analytical derivative methods in quantum chemistry to calculate the optimized molecular geometry and the vibrational frequencies of the molecules<sup>12-14</sup>. DFT method using the hybrid B3LYP functional is widely used for experimental structures and spectroscopic studies of various molecules<sup>15</sup>. Levosimendan molecule drew our attention since it bears a 6-phenyl 4,5-dihydro-3(2H)-pyridazinone ring which has easy functionalization at various ring positions. However, up to our best knowledge, although the numerous studies have been found in both medical and chemical literature dealing with the uses of levosimendan as a drug and with the syntheses

and evaluations of various pyridazinone derivatives, respectively, there is no sufficient study on its spectroscopic and quantum chemical properties.

The experimental and simulated IR and micro-Raman spectra and optimized molecular geometry, electronic absorption transition maximum wavelengths, HOMO-LUMO analysis, molecular electrostatic potential (MEP), natural bond orbital (NBO) analysis, thermodynamic properties and atomic charges of levosimendan by using the DFT/B3LYP method with 6-311++G(d,p) basis set in ground state, have been reported in the present paper.

### 2 Experimental Details

Levosimendan molecule, ( $C_{14}H_{12}N_6O$ ), used in this study was obtained from commercial source (Sigma-Aldrich; % 98) and used without any further purification.

IR spectrum of levosimendan was recorded at room temperature on a Perkin Elmer Spectrum on FT-IR (Fourier Transform Infrared) Spectrometer with a resolution of  $4\text{ cm}^{-1}$  in the transmission mode. The sample was compressed into self-supporting pellet and introduced into an IR cell equipped with KBr window.

The micro-Raman spectrum of title molecule was recorded by using a Jasco NRS-3100 micro-Raman Spectrophotometer (1800 lines/mm grating and high sensitivity cooled CCD) at room temperature in the region  $100-3600\text{ cm}^{-1}$ . The spectrometer was calibrated with the silicon phonon mode at  $520\text{ cm}^{-1}$

and microscope objective 100x was used. The 632.8 nm lines of HeNe laser was used for excitation. The exposure time was taken as 30 s and 10 scans were accumulated. The ultraviolet visible spectrum of the title compound was recorded by using a PG Instrument T80+ ultraviolet spectrophotometer at room temperature. The ultraviolet visible spectrum of the mentioned compound solved in ethanol was verified with spectral bandwidth 2 nm and quartz cell 1 cm.

### 3 Computational Details

In the present study, all calculations were carried out with GaussView 05 molecular visualization program and Gaussian 09 program package<sup>16,17</sup>. The molecular geometry and vibrational calculations of levosimendan were computed by using density functional theory Becke-3-Lee Yang Parr (B3LYP) method with 6-311++G(d,p) basis set in ground state<sup>18,19</sup>. It is well-known that the wavenumber values calculated at this level contain the well-known systematic errors<sup>20</sup>. That is why, the calculated vibrational wavenumbers were scaled as 0.983 for frequencies less than 1700 cm<sup>-1</sup> and 0.958 for frequencies higher than 1700 cm<sup>-1</sup> for B3LYP/6-311++G(d,p) basis set in levosimendan molecule<sup>21</sup>. The assignments of fundamental vibrational modes of the title molecule were performed on the basis of total energy distribution (TED) analysis by using VEDA 4 program<sup>22</sup>. The Raman activities ( $S_i$ ) calculated by using Gaussian 09 program have been converted to relative Raman intensities ( $I_i$ ) using the following relationship:

$$I_i = \frac{f(v_0 - v_i)^4 S_i}{v_i [1 - \exp(-hc\nu_i / kT)]} \quad \dots (1)$$

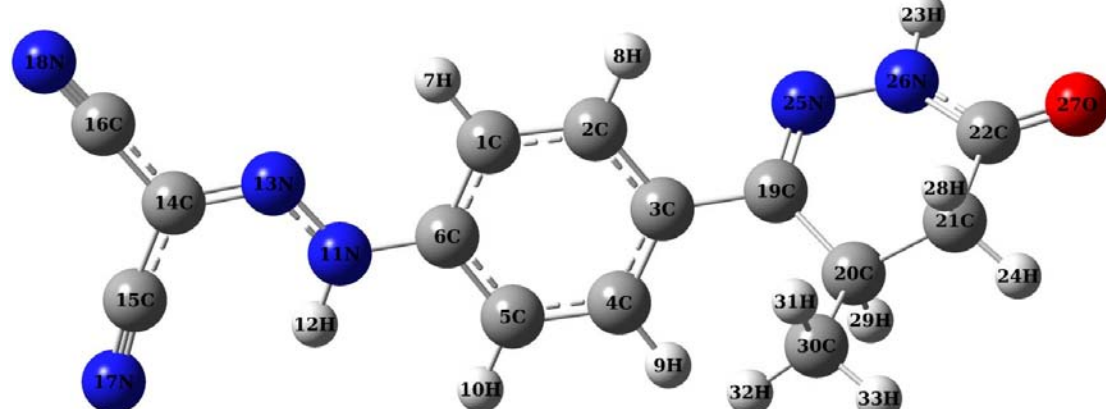


Fig. 1 — Numbering of the atoms and optimized structure of levosimendan molecule on B3LYP/6-311++G(d,p) basis set

where  $v_0(\text{cm}^{-1})$  is the exciting frequency,  $v_i$  is the vibrational wavenumber of the  $i^{\text{th}}$  normal mode,  $h$ ,  $c$ , and  $k$  are well-known universal constants and  $f$  is the suitably chosen common scaling factor for the peak intensities<sup>20,23</sup>.

### 4 Results and Discussion

#### 4.1 Molecular geometry

The optimized molecular structure of levosimendan is shown in Fig. 1. The optimized molecular geometry parameters of title molecule at B3LYP/6-311++G(d,p) level are listed in Table 1. Since the experimental parameters for the molecular structure of levosimendan do not exist in the literature, the only calculated molecular geometric parameters are presented in Table 1. Therefore, the calculated single (N25-N26) and double (N11=N13) bond lengths between two nitrogen atoms are found to be 1.371 Å and 1.303 Å, respectively. The triple bond lengths between C15≡N17 and C16≡N18 were found as 1.157 Å and 1.156 Å, respectively. These values are very satisfied due to the greater bond order and the shorter bond length. In the pyridazinone ring, the largest bond lengths between the atoms C20-C21, C20-C30 and C21-C22 were calculated as 1.540, 1.537 and 1.510 Å, respectively, while in the phenyl ring the bond lengths between carbon atoms were found to be at the interval 1.387 and 1.404 Å. Calculated results predict that in levosimendan, the largest bond angle of 127.444° becomes the angle C22-N26-N25 and C1-C6-N11-H12, N11-N13-C14-C16, N13-C14-C16-N18 and N25-N26-C22-O27 dihedral angle values were found to be about ± 179°. These results indicate that the title molecule is not planar.

Table 1 — Optimized molecular geometric parameters at B3LYP/6-311++G(d,p) level of levosimendan molecule

Atoms	Calculated bond lengths (Å)	Atoms	Calculated bond angles (°)	Atoms	Calculated dihedral angles (°)
C1-C2	1.387	C2-C1-C6	119.273	C1-C2-C3-C4	0.448
C1-C6	1.397	C2-C1-H7	120.847	C1-C2-C3-C19	177.172
C1-H7	1.082	C6-C1-H7	119.880	C1-C6-C5-C4	0.499
C2-C3	1.404	C1-C2-C3	121.600	C1-C6-N11-H12	179.235
C2-H8	1.083	C1-C2-H8	119.564	C1-C6-N11-N13	-0.431
C3-C4	1.401	C3-C2-H8	118.836	C2-C3-C19-C20	141.960
C3-C19	1.485	C2-C3-C4	118.081	C2-C3-C19-N25	-41.216
C4-C5	1.389	C2-C3-C19	120.207	C3-C19-C20-C21	-155.417
C4-H9	1.083	C4-C3-C19	121.628	C3-C19-C20-C30	-32.294
C5-C6	1.397	C3-C4-C5	121.024	C3-C19-C20-H29	88.026
C5-H10	1.085	C3-C4-H9	120.354	C4-C3-C19-C20	-41.435
C6-N11	1.409	C5-C4-H9	118.588	C4-C3-C19-N25	135.389
N11-H12	1.021	C4-C5-C6	119.808	C6-N11-N13-C14	176.679
N11-N13	1.303	C4-C5-H10	119.913	N11-N13-C14-C15	-0.065
N13-C14	1.312	C6-C5-H10	120.278	N11-N13-C14-C16	179.887
C14-C15	1.429	C1-C6-C5	120.211	N13-C14-C15-N17	0.072
C14-C16	1.425	C1-C6-N11	121.829	N13-C14-C16-N18	-179.124
C15-N17	1.157	C5-C6-N11	117.960	C14-N13-N11-H12	0.021
C16-N18	1.156	C6-N11-H12	117.741	C19-C20-C21-C22	-41.960
C19-C20	1.527	C6-N11-N13	122.134	C19-C20-C21-H24	-165.083
C19-N25	1.287	H12-N11-N13	120.124	C19-C20-C21-H28	79.956
C20-C21	1.540	N11-N13-C14	120.197	C19-N25-N26-C22	-15.712
C20-H29	1.101	N13-C14-C15	121.747	C19-N25-N26-H23	172.369
C20-C30	1.537	N13-C14-C16	118.583	C20-C21-C22-O27	-152.450
C21-C22	1.510	C15-C14-C16	119.671	C21-C22-N26-N25	-0.971
C21-H24	1.090	C3-C19-C20	122.425	N25-N26-C22-O27	-178.091
C21-H28	1.098	C3-C19-N25	114.848		
C22-N26	1.378	C20-C19-N25	122.648		
C22-O27	1.215	C19-C20-C21	109.393		
H23-N26	1.010	C19-C20-H29	106.598		
N25-N26	1.371	C19-C20-C30	115.069		
C30-H31	1.094	C21-C20-H29	108.017		
C30-H32	1.089	C21-C20-C30	109.038		
C30-H33	1.093	H29-C20-C30	108.493		
		C20-C21-C22	114.205		
		C20-C21-H24	111.411		
		C20-C21-H28	109.370		
		C22-C21-H24	108.321		
		C22-C21-H28	106.264		
		H24-C21-H28	106.903		
		C21-C22-N26	113.266		
		C21-C22-O27	124.977		
		N26-C22-O27	121.689		
		C19-N25-N26	119.100		
		C22-N26-H23	117.789		
		C22-N26-N25	127.444		
		H23-N26-N25	114.301		
		C20-C30-H31	110.662		
		C20-C30-H32	113.054		
		C20-C30-H33	109.557		
		H31-C30-H32	107.756		
		H31-C30-H33	107.844		
		H32-C30-H33	107.791		

#### 4.2 Vibrational frequencies

Levosimendan has 33 atoms and 93 normal vibrational modes which are active in both infrared and Raman. The experimental and simulated IR and micro-Raman spectra of levosimendan molecule are given in Fig. 2(a and b) and Fig. 3(a and b), respectively. Furthermore, the calculated vibrational wavenumbers at B3LYP/6-311++G(d,p) and their assignments are presented in Table 2.

#### 4.2.1 N-H, C≡N and C-N vibrations

It is well-known that the heteroaromatics including a N-H group exhibits its stretching vibration<sup>24,25</sup> in the region 3520–3320 cm<sup>-1</sup>. In our study, the observed peak at 3337 cm<sup>-1</sup> (IR) and two weak bands at 3508 (R) cm<sup>-1</sup> and 3337 (R) cm<sup>-1</sup> can be attributed to the ν(N-H) modes. The stretching C≡N vibrational bands of nitrile groups in levosimendan are observed at 2224 s (IR)-2223vs (R) cm<sup>-1</sup> and 2213 sh (IR)-

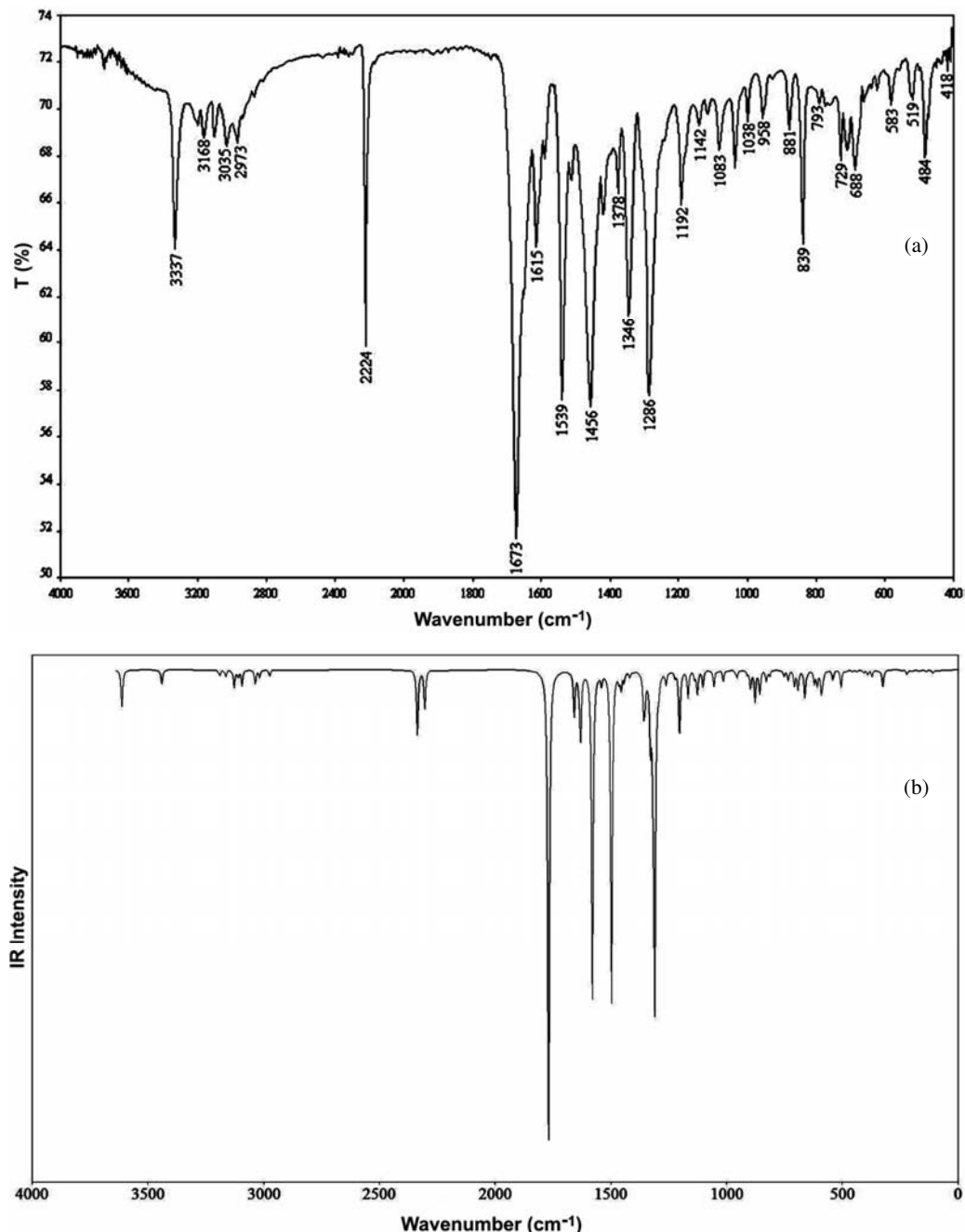


Fig. 2 — Experimental IR spectrum (a) and the calculated IR spectrum on B3LYP/6-311++G(d,p) basis set (b) of levosimendan molecule

2212 s (R)  $\text{cm}^{-1}$  (Ref. 26). Furthermore, the v(C-N) stretching modes of aromatic rings in levosimendan are observed at 1286 s (IR)-1291 vs (R)  $\text{cm}^{-1}$  and 1192 m (IR)-1192 w (R)  $\text{cm}^{-1}$  which are found to be in good agreement with the calculated values<sup>22</sup> as seen in Table 2. Similarly, the NHH and CNN deformation bands of title molecule are observed at 1606 sh (IR)-1598 vs (R)  $\text{cm}^{-1}$ , 1540 s (IR)-1546 w (R)  $\text{cm}^{-1}$

and 881 m (IR)-882 m (R)  $\text{cm}^{-1}$  which are also in a good agreement with the calculated values as seen in Table 2.

#### 4.2.2 C-H, C=O and C-C vibrations

By considering Figs. 2(a) and 3(a) and Table 2, the C-H stretching bands of phenyl ring of title molecule are observed in the range 3199-3035 (IR) and

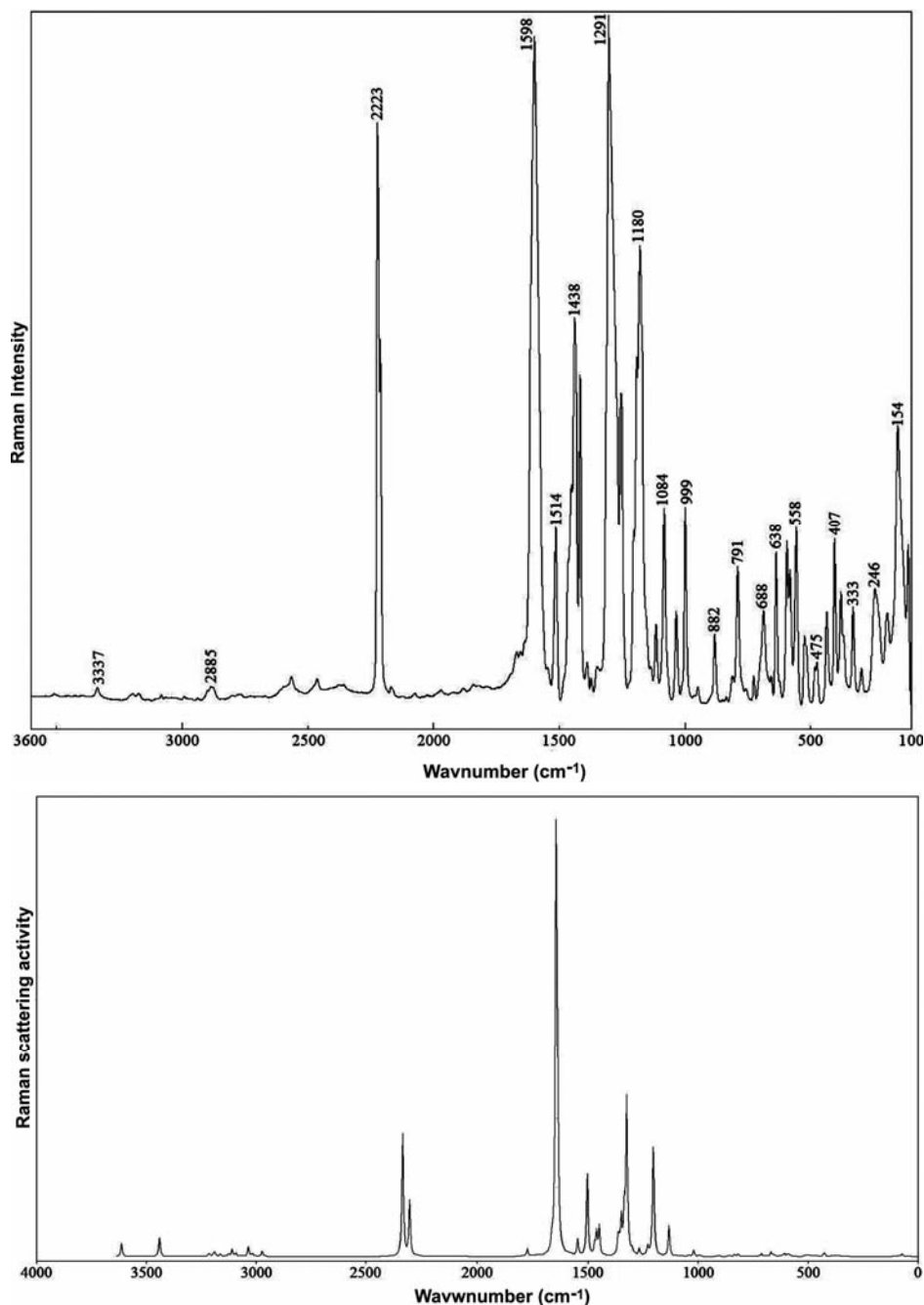


Fig. 3 — Experimental micro-Raman spectrum (on top) and the calculated micro-Raman spectrum on B3LYP/6-311++G(d,p) basis set (on bottom) of levosimendan molecule

Table 2 — Observed IR and Raman frequencies, calculated frequencies, relative intensities and probable assignments of levosimendan molecule

Assignments	Experimental ( $\text{cm}^{-1}$ )		Calculated at B3LYP/6-311++G(d,p)			
	IR	Raman	Unscaled	Scaled	$I_{\text{IR}}$	$S_{\text{Raman}}$
Lattice mode			21,35	20,99	0,917	3,805
Lattice mode			26,28	25,83	0,907	1,541
Lattice mode			36,52	35,90	1,814	4,538
Lattice mode			57,46	56,49	1,011	1,966
Lattice mode			69,48	68,30	0,519	24,837
Lattice mode			89,73	88,21	1,294	1,898
$\delta\text{NCC}+\delta\text{CCC}+\tau\text{NCCC}$			104,18	102,40	2,442	5,882
$\delta\text{NCC}+\delta\text{CCC}+\tau\text{CNNN}$	111 m		108,86	107,01	3,988	2,167
$\tau\text{NCCN}+\tau\text{CNNN}+\gamma\text{CNCC}+\tau\text{CH}_3$			136,19	133,87	3,448	6,155
$\tau\text{CH}_3+\tau\text{NCCN}+\tau\text{CNNN}+\gamma\text{CNCC}+\tau\text{CCCC}$	154 s		171,44	168,52	2,363	2,660
$\tau\text{CH}_3$		197 m	200,44	197,04	0,757	2,490
$\tau\text{CH}_3$			202,26	198,83	1,509	2,734
$\tau\text{CH}_3+\delta\text{NCC}+\delta\text{CCN}+\delta\text{CCC}$			221,29	217,53	6,948	8,504
$\tau\text{CH}_3+\tau\text{CNNC}+\tau\text{CCCC}$	246 m		244,38	240,23	1,391	1,565
$\delta\text{C-C-CH}_3$		299 w	312,59	307,28	0,657	0,491
$\tau\text{NCCN}+\tau\text{CNNN}+\gamma\text{CNCC}$			325,13	319,60	25,177	0,919
$\tau\text{CNNC}+\gamma\text{CCCC}$	333 m		342,64	336,82	1,626	7,211
$\delta\text{NCC}+\delta\text{CNN}+\delta\text{CCC}$		372 sh	371,17	364,86	10,223	9,042
$\tau\text{CCCC}+\gamma\text{NCCC}$		380 m	390,24	383,60	6,661	9,936
$\delta\text{NCC}+\delta\text{CNN}+\delta\text{CCC}+\gamma\text{NCCC}$	409 w	407 s	407,00	400,08	4,478	4,045
$\tau\text{CCCC}$	418 w		420,38	413,23	0,794	38,408
$\delta\text{CCN}+\delta\text{CCC}+\delta\text{OCN}$		437 m	437,25	429,82	2,869	4,270
$\delta\text{CCN}+\delta\text{CCC}+\delta\text{OCN}$	453 w		455,69	447,94	2,913	11,469
$\tau\text{NCCN}+\tau\text{CNNN}$	484 s	482 w	486,43	478,16	2,975	3,768
$\tau\text{CCCC}+\tau\text{HNNC}+\tau\text{HCCC}+\delta\text{OCN}$	501 w		505,28	496,69	25,634	19,327
$\tau\text{CCCC}+\gamma\text{NCCC}+\tau\text{HCCC}+\rho\text{CH}_2$	519 m	526 m	540,94	531,74	15,138	5,298
$\delta\text{NCC}+\delta\text{CCN}+\nu\text{NC}$	559 w	558 s	578,60	568,77	3,005	13,242
$\tau\text{HNNC}+\tau\text{HCCC}$			585,86	575,90	16,112	21,162
$\tau\text{HNNC}+\gamma\text{OCNC}$	583 m	583 m	591,00	580,95	28,259	2,202
$\delta\text{NC-C-NC}$			601,47	591,25	1,048	28,016
$\tau\text{HNNC}+\gamma\text{CNCC}$		596 s	608,73	598,38	21,090	9,436
$\tau\text{HNNC}+\rho\text{CH}_2+\gamma\text{OCNC}$	624 w	624 sh	621,27	610,71	18,445	9,401
$\delta\text{CCC}+\tau\text{HNNC}$	641 w	638 s	650,91	639,84	4,650	21,841
$\tau\text{HNNC}+\gamma\text{OCNC}+\tau\text{NCCC}$	663 w	658 w	661,87	650,62	38,507	54,034
$\tau\text{HNNC}+\gamma\text{CNCC}+\tau\text{NCCN}$	688 m	688 m	691,42	679,66	28,786	2,335
$\delta\text{CCC}+\nu\text{CC}+\rho\text{CH}_2+\delta\text{CCN}$	711 m	702 sh	706,79	694,78	22,919	36,570
$\tau\text{CCCC}+\gamma\text{CCCC}+\delta\text{CNN}+\rho\text{CH}_2$	729 m	728 w	733,92	721,44	14,338	6,544
$\tau\text{CCCC}+\gamma\text{CCCC}+\delta\text{CNN}+\rho\text{CH}_2$	762 w	761 w	752,52	739,72	8,847	3,832
$\delta\text{NC-C-NC}+\delta\text{CCC}+\nu\text{CC}+\nu\text{NC}$	793 w	791 s	813,92	800,08	8,460	27,951
$\tau\text{HCCC}$		813 w	828,32	814,24	15,747	31,018
$\tau\text{HCCC}$	839 s	836 w	856,88	842,31	33,333	10,846
$\rho\text{CH}_3+\rho\text{CH}_2+\nu\text{CC}+\nu\text{NC}$			877,02	862,11	44,760	1,820
$\delta\text{CNN}+\nu\text{CC}+\delta\text{CCC}$	881 m	882 m	896,54	881,29	26,406	11,032
$\delta\text{H-C-CH}_3+\rho\text{CH}_3+\nu\text{C-CH}_2$			909,76	894,30	6,431	5,258
$\rho\text{CH}_3+\nu\text{C-CH}_2+\tau\text{HCCN}$	928 w		954,84	938,60	10,708	4,687
$\tau\text{HCCC}$	950 w	950 w	960,90	944,57	3,164	1,366
$\tau\text{HCCC}$	958 m	963 vw	989,56	972,73	0,129	14,630
$\delta\text{CCC}+\delta\text{CCN}+\rho\text{CH}_3$	1000 m	999 s	1013,93	996,69	17,230	74,954
$\delta\text{HCC}+\nu\text{CC}$			1035,24	1017,64	1,838	22,969
$\nu\text{C-CH}_3+\rho\text{CH}_3+\rho\text{CH}_2$	1038 m	1035 m	1054,52	1036,59	24,797	7,255
$\nu\text{C-CH}_3+\rho\text{CH}_3+\rho\text{CH}_2$	1083 m	1084 s	1101,98	1083,25	23,951	4,501
$\nu\text{NN}+\nu\text{CC}+\rho\text{CH}_3+\delta\text{HCC}$			1126,10	1106,96	34,556	361,026
$\delta\text{HCC}+\tau\text{HCCN}+\nu\text{CC}$	1116 w		1138,40	1119,05	10,849	1,092
$\delta\text{HCC}+\nu\text{NN}+\nu\text{CC}+\tau\text{HCCN}$	1142 m	1136 w	1166,63	1146,80	38,669	1,892
$\delta\text{HCC}$		1160 m	1197,07	1176,72	1,854	1343,148

*Contd —*

Table 2 — Observed IR, Raman frequencies, calculated frequencies, relative intensities and probable assignments of levosimendan molecule — *Contd*

Assignments	Experimental ( $\text{cm}^{-1}$ )		Calculated at B3LYP/6-311++G(d,p)			
	IR	Raman	Unscaled	Scaled	$I_{\text{IR}}$	$S_{\text{Raman}}$
$\tau\text{CH}_2+\delta\text{HCC}+\nu\text{NC}$	1181 sh	1180 s	1203,20	1182,75	93,810	20,020
$\nu\text{NC}+\delta\text{HCC}+\nu\text{C-CN}+\nu\text{NN}+\nu\text{CC}$	1192 m	1192 w	1222,52	1201,74	8,851	116,485
$\nu\text{C-CN}+\delta\text{CNN}+\delta\text{HCC}+\delta\text{HNN}+\nu\text{CC}$	1243 w	1255 s	1261,24	1239,79	17,831	84,946
$\delta\text{HCC}+\nu\text{CH}_2$			1293,58	1271,59	18,338	67,152
$\nu\text{NC}+\nu\text{NN}+\delta\text{HCC}$	1286 s	1291 vs	1310,74	1288,46	500,669	96,825
$\nu\text{CC}+\nu\text{CH}_2+\delta\text{HCC}$			1317,12	1294,72	24,072	18,064
$\nu\text{NN}+\nu\text{CH}_2+\delta\text{HNN}+\delta\text{HCC}$			1318,06	1295,65	79,607	1838,473
$\nu\text{CC}+\delta\text{HCC}$	1311 sh		1328,92	1306,33	94,006	522,408
$\nu\text{CC}+\delta\text{HCC}$			1342,71	1319,88	3,718	444,175
$\tau\text{HCCN}$			1351,84	1328,86	28,644	103,072
$\nu\text{CH}_2+\delta\text{HCC}$	1346 s	1349 w	1357,61	1334,53	60,663	216,015
$\delta\text{CH}_3$	1378 m	1374 w	1418,71	1394,59	8,416	7,521
$\nu\text{CC}+\delta\text{HCC}+\delta\text{HNN}$	1420 m	1417 s	1442,52	1417,99	13,238	363,947
$\delta\text{HNC}+\delta\text{CH}_2$			1455,12	1430,39	23,094	287,421
$\delta\text{CH}_2+\delta\text{HNC}$		1438 s	1464,24	1439,35	11,567	129,851
$\nu\text{N=C}+\delta\text{HNN}+\delta\text{HCC}$			1497,04	1471,59	470,032	1052,756
$\delta_s\text{CH}_3$	1456 s	1451 w	1498,63	1473,15	8,398	8,280
$\delta_s\text{CH}_3$	1467 sh	1465 sh	1502,75	1477,20	14,496	15,544
$\nu\text{CC}+\delta\text{HCC}+\nu\text{NC}$	1513 m	1514 m	1540,73	1514,54	17,109	220,638
$\delta\text{HNN}+\nu\text{N=C}+\nu\text{CC}+\delta\text{HCC}$	1540 s	1546 w	1579,44	1552,59	495,588	16,773
$\delta\text{HNN}+\delta\text{HCC}+\nu\text{CC}+\nu\text{N=C}$	1606 sh	1598 vs	1630,82	1603,10	104,535	1664,640
$\nu\text{CC}+\nu\text{N=C}+\delta\text{HCC}+\delta\text{HNC}+\delta\text{HNN}$	1615 s		1638,44	1610,58	12,833	5520,164
$\nu\text{CC}+\nu\text{N=C}+\delta\text{HCC}+\delta\text{HNC}+\delta\text{HNN}$			1658,20	1630,01	63,392	145,557
$\nu\text{O=C}+\delta\text{HNC}$	1674 vs	1669 w	1768,96	1694,67	716,318	105,219
$\nu\text{N=C}$	2213 sh	2212 s	2303,86	2207,10	57,883	861,078
$\nu\text{N=C}$	2224 s	2223 vs	2335,66	2237,57	94,507	1911,304
$\nu\text{CH}$	2823 w	2842 vw	2974,25	2849,34	9,003	103,545
$\nu_s\text{CH}_2$	2872 w	2885 w	3016,76	2890,05	10,359	58,562
$\nu_s\text{CH}_3$		2897 sh	3035,90	2908,40	20,843	182,989
$\nu_{as}\text{CH}_3$	2938 w	2937 w	3093,45	2963,52	22,908	64,371
$\nu_{as}\text{CH}_2$	2974 m	2982 vw	3110,09	2979,47	9,808	137,499
$\nu_{as}\text{CH}_3$		2992 w	3127,01	2995,67	25,140	45,719
$\nu\text{CH}$	3035 m	3041 vw	3163,61	3030,74	9,842	53,227
$\nu\text{CH}$	3102 m	3083 w	3189,54	3055,58	8,007	87,763
$\nu\text{CH}$	3168 m	3174 w	3198,44	3064,11	1,294	40,826
$\nu\text{CH}$	3199 m	3197 w	3215,61	3080,55	0,027	60,093
$\nu\text{NH}$	3337 s	3337 w	3440,00	3295,52	20,792	393,289
$\nu\text{NH}$		3508 w	3612,17	3460,46	57,470	287,795

v, stretching;  $\delta$ , bending;  $\delta_s$ , scissoring;  $\rho$ , rocking;  $\gamma$ , out-of-plane bending;  $\tau$ , torsion; s, strong; m, medium; w, weak; v, very; sh, shoulder. IR intensities (km/mole);  $S_R$ , Raman scattering activities ( $\text{\AA}^4/\text{amu}$ ).

3197-3041 (R)  $\text{cm}^{-1}$  while the symmetric  $\nu(\text{C}-\text{H})$  bands<sup>27,28</sup> arise at 2823 w (IR) and 2842 vw (R)  $\text{cm}^{-1}$ . Likewise, the asymmetric and symmetric stretching bands of  $\text{CH}_3$  methyl group of pyridazinone ring can be attributed to the observed peaks at 2992 w (R) and 2938 w (IR)-2937w (R)  $\text{cm}^{-1}$  and 2897 sh (R)  $\text{cm}^{-1}$ , respectively. Whereas the asymmetric and symmetric stretching modes of  $\text{CH}_2$  methylene group in pyridazinone ring of levosimendan are observed at 2974 m (IR)-2982 vw (R)  $\text{cm}^{-1}$  and 2872 w (IR)-2885 w (R)  $\text{cm}^{-1}$ , respectively<sup>28,29</sup>. The deformation, rocking and torsional modes of  $\text{CH}_3$  group are

observed at 1467 sh (IR)-1465 sh (R)  $\text{cm}^{-1}$  and 1456 s (IR)-1451 w (R)  $\text{cm}^{-1}$  and 928 w (IR)  $\text{cm}^{-1}$  and 246 m, 197 m and 154 s  $\text{cm}^{-1}$  in the micro-Raman spectrum of title molecule, respectively. Similarly, the  $\text{C}-\text{CH}_3$  stretching bands arise at 1083 m (IR)-1084 s (R)  $\text{cm}^{-1}$  and 1038 m (IR)-1035 m (R)  $\text{cm}^{-1}$ . The exhibit peak at 1674 vs (IR)-1669 w (R)  $\text{cm}^{-1}$  can be attributed to the  $\text{C=O}$  stretching absorption band of pyridazinone ring in levosimendan<sup>10,11</sup>. Likewise, the  $\nu(\text{C}-\text{C})$  stretching bands of aromatic rings can be assigned to the observed peaks<sup>24</sup> at 1615 s (IR)  $\text{cm}^{-1}$  and 1420 m (IR)-1417 s (R)  $\text{cm}^{-1}$ .

Table 3 — Experimental and calculated absorption wavelength ( $\lambda$ ), excitation energies and oscillator strengths ( $f$ ) of levosimendan molecule

Exp. $\lambda$ (nm) (in ethanol)	Transition	Calculated at B3LYP/6-311++G(d,p) level in vacum / ethanol		
		$\lambda$ (nm) in ethanol	Excitation energy (eV)	$f$ (oscillator strength)
415 and 401		393.16 / 407.90	3.1535 / 3.0396	0.6099 / 0.7661
-		324.74 / 320.09	3.8179 / 3.8734	0.0286 / 0.1501
-		310.34 / 314.62	3.9952 / 3.9408	0.2555 / 0.0532
-		298.56 / 303.86	4.1527 / 4.0804	0.0217 / 0.0566
289		280.69 / 283.32	4.4172 / 4.3761	0.2075 / 0.2498
218 and 249		269.63 / 270.23	4.5983 / 4.5881	0.0122 / 0.0002

#### 4.3 UV-Vis. Absorption and FMOs analysis

Table 3 exhibits the experimental maximum absorption wavelengths ( $\lambda_{\max}$ ) in ethanol solvent and the calculated maximum absorption wavelengths ( $\lambda_{\max}$ ), excitation energies and oscillator strengths ( $f$ ) of levosimendan molecule in both vacuum and ethanol which were calculated by using TD-DFT/B3LYP method with 6-311++G(d,p) basis set in ground state. Therefore, the observed  $\lambda_{\max}$  values of levosimendan in ethanol at 218 and 249 nm can be assigned to the  $n \rightarrow \sigma^*$  transition while the  $\lambda_{\max}$  value at 289 nm can be attributed to the  $\pi \rightarrow \pi^*$  transition and finally the values at 401 and 415 nm indicate the  $n \rightarrow \pi^*$  transition<sup>30</sup>. A comparison between experimental and calculated  $\lambda_{\max}$  values of levosimendan in ethanol solvent exhibits a good agreement for the values at (exp/cal) 289/283.32 nm, 415 and 401/407.90 nm as seen in Table 2.

The formed energy gaps between the highest occupied molecular orbital (HOMO) and lowest unoccupied molecular orbital (LUMO) called the frontier molecule orbitals (FMOs) which are the main orbital taking part in chemical reaction which indicate the molecular chemical stability<sup>31,32</sup>. The 3D plots and energy difference for title molecule are shown in Fig. 4.

#### 4.4 NBO analysis

Natural bond orbital (NBO) analysis emphasises on the role of intermolecular orbital interaction in a molecule<sup>33</sup>. It is carried out by considering all possible interactions between filled donor and empty acceptor NBOs and estimating their energetic importance by second order perturbation theory<sup>34</sup>. The results of second order perturbation theory analysis of Fock matrix at B3LYP/6-311++G(d,p) level for levosimendan are given in Table 4.

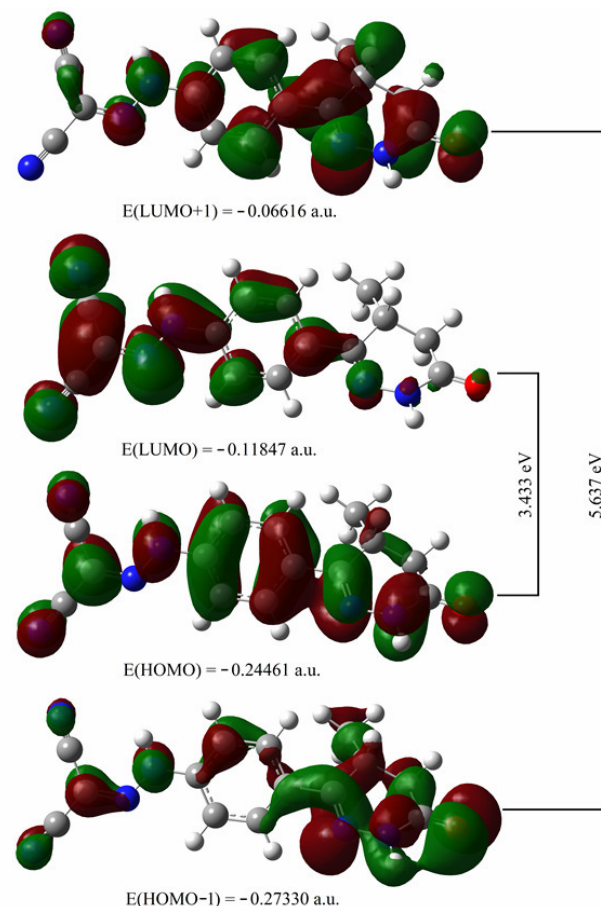


Fig. 4 — 3D plots of HOMOs and LUMOs of levosimendan molecule on B3LYP/6-311++G(d,p) basis set

Therefore, we can easily state by considering Table 4 that the highest energy values of hyperconjugative interactions in levosimendan arised at the transition between  $n$  electrons of N11 atom and  $\pi^*$  of N13-C14 bonding (i.e.  $n_{N11} \rightarrow \pi^*_{N13-C14}$ ) and similarly,  $n_{N26} \rightarrow \pi^*_{C22-O27}$ ,  $n_{N11} \rightarrow \pi^*_{C5-C6}$  and  $n_{N26} \rightarrow \pi^*_{C19-N25}$  which correspond to the  $n \rightarrow \pi^*$  transition given in Table 3. Likewise, the  $\pi_{C1-C2} \rightarrow \pi^*_{C5-C6}$ ,  $\pi_{C3-C4} \rightarrow \pi^*_{C5-C6}$ ,  $\pi_{N13-C14} \rightarrow \pi^*_{C15-N17}$  and

$\pi_{N13-C14} \rightarrow \pi^*_{C16-N18}$  transitions correspond to the  $\pi \rightarrow \pi^*$  transition given in Table 3 and finally,  $n_{O27} \rightarrow \sigma^*_{C22-N26}$  and  $n_{O27} \rightarrow \sigma^*_{C21-C22}$  transitions correspond to the  $n \rightarrow \sigma^*$  transition in Table 3. Therefore, the NBO analysis in another way provides a confirmation of HOMO-LUMO and UV-Vis. analyses.

#### 4.5 Molecular electrostatic potential (MEP), thermodynamic properties and atomic charges

It is well known that the Molecular Electrostatic Potential (MEP) is a crucial concept to understand the molecular interactions in a given molecule and at the same time it is used for interpreting and predicting

Table 4 — Second order perturbation theory of Fock matrix in NBO of levosimendan molecule

Donor (i)	ED(i)(e)	Acceptor (j)	ED(j)(e)	E(2) <sup>a</sup> kcal mol <sup>-1</sup>	E(j)-E(i) <sup>b</sup> a.u.	F(i,j) <sup>c</sup> a.u.
BD(1) C1-C2	1.97565	BD*(1) C6-N11	0.03142	4.46	1.10	0.062
BD(2) C1-C2	1.67383	BD*(2) C3-C4	0.36945	18.62	0.28	0.066
BD(2) C1-C2	1.67383	BD*(2) C5-C6	0.40894	22.92	0.27	0.071
BD(1) C1-C6	1.97124	BD*(1) C5-C6	0.02125	4.63	1.27	0.068
BD(1) C1-H7	1.97645	BD*(1) C5-C6	0.02125	4.42	1.07	0.062
BD(1) C2-H8	1.97807	BD*(1) C3-C4	0.02460	4.61	1.07	0.063
BD(2) C3-C4	1.63855	BD*(2) C1-C2	0.29201	19.74	0.29	0.068
BD(2) C3-C4	1.63855	BD*(2) C5-C6	0.40894	20.81	0.27	0.067
BD(2) C3-C4	1.63855	BD*(2) C19-N25	0.18710	10.47	0.29	0.051
BD(1) C3-C19	1.96599	BD*(1) N25-N26	0.02739	5.49	1.02	0.067
BD(1) C4-H9	1.97916	BD*(1) C2-C3	0.02376	4.26	1.09	0.061
BD(1) C5-C6	1.97206	BD*(1) C1-C6	0.02363	4.52	1.27	0.068
BD(2) C5-C6	1.64823	BD*(2) C1-C2	0.29201	16.62	0.30	0.064
BD(2) C5-C6	1.64823	BD*(2) C3-C4	0.36945	20.36	0.30	0.070
BD(1) C5-H10	1.97719	BD*(1) C1-C6	0.02363	4.41	1.09	0.062
BD(2) N13-C14	1.86026	BD*(2) N13-C14	0.38686	6.23	0.32	0.042
BD(2) N13-C14	1.86026	BD*(3) C15-N17	0.08860	16.24	0.44	0.076
BD(2) N13-C14	1.86026	BD*(3) C16-N18	0.09051	16.22	0.46	0.078
BD(1) C14-C15	1.97894	BD*(1) C15-N17	0.01000	6.81	1.66	0.095
BD(1) C14-C15	1.97894	BD*(1) C16-N18	0.01004	4.26	1.68	0.076
BD(1) C14-C16	1.97404	BD*(1) N11-N13	0.01522	4.03	1.18	0.062
BD(1) C14-C16	1.97404	BD*(1) C15-N17	0.01000	4.48	1.65	0.077
BD(1) C14-C16	1.97404	BD*(1) C16-N18	0.01004	7.42	1.67	0.100
BD(1) C15-N17	1.99421	BD*(1) C14-C15	0.04569	6.25	1.54	0.088
BD(3) C15-N17	1.96001	BD*(2) N13-C14	0.38686	9.12	0.32	0.053
BD(1) C16-N18	1.99400	BD*(1) C14-C16	0.03730	6.91	1.53	0.093
BD(3) C16-N18	1.96086	BD*(2) N13-C14	0.38686	9.28	0.30	0.052
BD(2) C19-N25	1.93468	BD*(2) C3-C4	0.36945	5.74	0.37	0.044
LP(1) N11	1.58674	BD*(2) C5-C6	0.40894	30.62	0.31	0.087
LP(1) N11	1.58674	BD*(2) N13-C14	0.38686	58.56	0.26	0.110
LP(1) N13	1.91073	BD*(1) N11-H12	0.04329	10.48	0.75	0.080
LP(1) N13	1.91073	BD*(1) C14-C15	0.04569	9.74	0.89	0.084
LP(1) N17	1.97134	BD*(1) C14-C15	0.04569	10.79	1.00	0.093
LP(1) N18	1.97192	BD*(1) C14-C16	0.03730	11.33	1.00	0.095
LP(1) N25	1.92661	BD*(1) C19-C20	0.04480	10.45	0.77	0.081
LP(1) N25	1.92661	BD*(1) C22-N26	0.09067	9.01	0.82	0.077
LP(1) N26	1.66603	BD*(2) C19-N25	0.18710	26.80	0.30	0.083
LP(1) N26	1.66603	BD*(2) C22-O27	0.25547	52.45	0.30	0.114
LP(2) O27	1.86141	BD*(1) C21-C22	0.06037	18.60	0.64	0.100
LP(2) O27	1.86141	BD*(1) C22-N26	0.09067	26.70	0.69	0.123
BD*(2) C5-C6	0.40894	BD*(2) C1-C2	0.29201	148.65	0.02	0.081
BD*(2) C5-C6	0.40894	BD*(2) C3-C4	0.36945	196.77	0.02	0.082
BD*(2) N13-C14	0.38686	BD*(3) C15-N17	0.08860	17.41	0.12	0.085
BD*(2) N13-C14	0.38686	BD*(3) C16-N18	0.09051	14.06	0.14	0.082

ED is the electron density.

<sup>a</sup> E(2) is the energy of hyperconjugative interactions.

<sup>b</sup> Energy difference between donor and acceptor i and j NBO orbitals.

<sup>c</sup> F(i,j) is the Fock matrix element between i and j NBO orbitals.

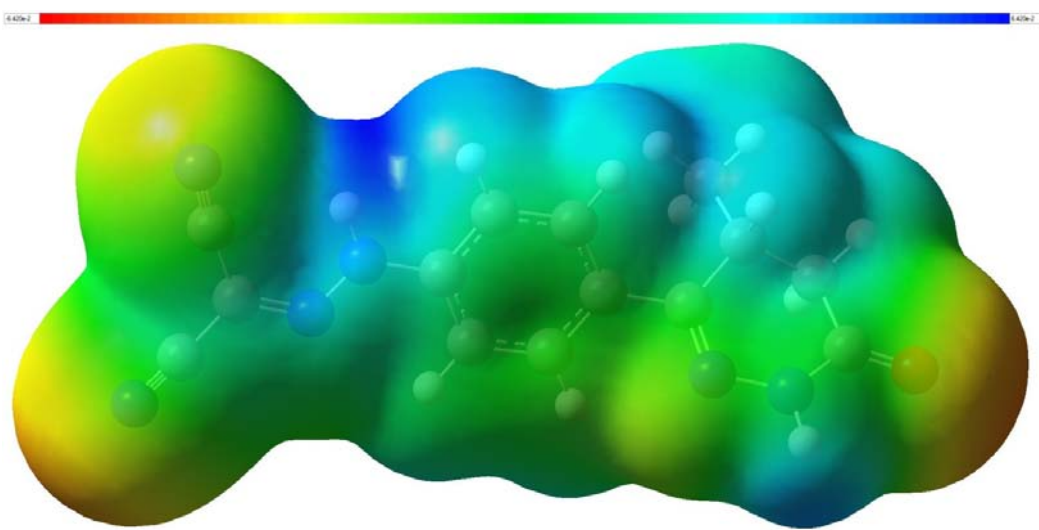


Fig. 5 — 3D plot of MEP of levosimendan molecule on B3LYP/6-311++G(d,p) basis set

Table 5 — Calculated thermodynamic properties and atomic charges of levosimendan molecule

Parameters	Value	Atoms	Mulliken atomic charges (a.u.)	NBO atomic charges (a.u.)
Thermal energy, E (cal/mol K)	167.086	C1	0.00579	-0.21258
Heat capacity, C <sub>v</sub> (cal/mol K)	70.475	C2	0.02597	-0.14367
Entropy, S (cal/mol K)	145.933	C3	0.81608	-0.07735
Dipol moment, D (Debye)		C4	-0.60887	-0.17413
μ <sub>x</sub>	3.4081	C5	-0.46430	-0.21853
μ <sub>y</sub>	-3.6319	C6	-0.57227	0.14359
μ <sub>z</sub>	0.2963	H7	0.23746	0.23531
μ <sub>total</sub>	4.9894	H8	0.22282	0.22420
		H9	0.20735	0.21035
		H10	0.14784	0.21139
Rotational constants (GHz)		N11	0.08649	-0.32049
A	1.01801	H12	0.26732	0.38013
B	0.10066	N13	0.11687	-0.12793
C	0.09488	C14	0.66149	-0.08491
Zero-point vibrational energy (kcal/mol)	155.26587	C15	-0.39025	0.23842
Sum of electronic and zero-point energy (Hartree/particle)	-944.366912	C16	-0.16906	0.26649
		N17	-0.24290	-0.28249
		N18	-0.22560	-0.27744
Sum of electronic and thermal Energies (Hartree/particle)	-944.348076	C19	-0.67570	0.23525
		C20	0.67169	-0.26948
		C21	-0.47841	-0.46527
Sum of electronic and thermal Enthalpies (Hartree/particle)	-944.347131	C22	0.05605	0.67320
		H23	0.33709	0.39978
		H24	0.22686	0.23661
Sum of electronic and thermal Free Energies (Hartree/particle)	-944.416469	N25	0.05370	-0.25990
		N26	-0.13944	-0.44179
		O27	-0.29657	-0.59404
Zero-point correction (Hartree/particle)	0.247432	H28	0.20582	0.22681
Thermal correction to Energy (Hartree/particle)	0.266268	H29	0.21197	0.21492
Thermal correction to Enthalpy (Hartree/particle)	0.267213	C30	-0.72937	-0.56693
Thermal correction to Gibbs Free Energy (Hartree/particle)	0.197875	H31	0.16907	0.20421
E(RB+HF-LYP)	-944.61434404	H32	0.12057	0.20894
		H33	0.14444	0.20732

relative reactivities sites for electrophilic and nucleophilic attack, investigation of biological recognition, hydrogen bonding interactions, studies of zeolite, molecular cluster, crystal behaviour, correlation and prediction of a wide range of macroscopic properties<sup>35,36</sup>.

Figure 5 shows the 3D plot of the MEP which was calculated by using the optimized molecular structure at B3LYP/6-311++G(d,p) level for levosimendan molecule. In Fig. 5, the electrostatic potentials at the surface are shown by different colours. Therefore, the red colour parts represent the regions of negative electrostatic potential, the blue ones represent the regions of positive electrostatic potential and green colour parts also represent the regions of zero potential. Furthermore, the negative regions (red colour) of MEP are related to electrophilic reactivity and the positive ones (blue colour) are related to nucleophilic reactivity.

The atomic charge in molecules is used for descriptions of the charge transfer and electronegativity in chemistry<sup>37</sup>. Likewise, the thermodynamical data obtained from the quantum chemical calculations are often used in the reaction mechanism of the organic compound. In this framework, the results of the calculations of Mulliken<sup>38</sup>, NBO atomic charges and thermodynamic parameters (such as thermal energy, entropy, heat capacity, dipole moment, rotational constants and zero-point energy (ZPE)) for the levosimendan molecule at B3LYP/6-311++G(d,p) level are presented in Table 5. By considering the data given in Table 5, the highest positive atomic charges were found as 0.81608 au, 0.67165 au and 0.33709 au for the C3 carbon atom in phenyl ring and H23 hydrogen and C20 carbon atoms in the pridazinone ring of the mentioned molecule, respectively. The thermal energy value for the levosimendan molecule was calculated as 167.086 cal/mol K.

## 5 Conclusions

In the present study, molecular structure, vibrational frequencies, UV-vis maximum wavelengths, HOMO and LUMO analysis, NBO analyses, molecular electrostatic potential (MEP), thermodynamic properties and atomic charges of levosimendan molecule have been calculated by using DFT/B3LYP method with 6-311++ G(d,p) basis set in ground state. The calculated vibrational frequency and electronic absorption wavelength

values (in ethanol) are found to be in good agreement with the experimental data. The results obtained from this study can be considered for other cardionic agents bearing a 6-phenyl-4,5-dihydro-3-(2H)-pyridazinone ring.

## Acknowledgement

This work was supported by Turkish Scientific and Technological Research Council (TÜBİTAK) (Project No: 111T683).

## References

- 1 Follath F, Cleland J G F, Just H, Papp J G Y, Scholz H, Peuhkurinen K, Harjola V P, Mitrovic V, Abdalla M, Sandell E P & Lehtonen L, *Lancet*, 360 (2002) 196.
- 2 Moiseyev V S, Pöder P, Andrejevs N, Ruda M Y, Golikov A P, Lazebnik L B, Kobalava Z D, Lehtonen L A, Laine T, Nieminen M S & Liek I, *European Heart Journal*, 23 (2002) 1422.
- 3 Nieminen M S, Akkila J, Hasenfuss G, Kleber F X, Lehtonen L A, Mitrovic V, Nyquist O & Remme W J, *J Am Coll Cardiol*, 36 (2000) 1903.
- 4 Bowman P, Haikala H & Paul R J, *J Pharmac Exp Ther*, 288 (1999) 316.
- 5 Ukkonen H, Saraste M, Akkila J, Knuuti J, Karanko M, Iida H, Lehikoinen P, Någren K, Lehtonen L & Voipio-Pulkki L M, *Clin Pharmacol Ther*, 68 (2000) 522.
- 6 Sandell E P, Häyhä M, Antila S, Heikkilä P, Ottoila P, Lehtonen L A & Penttiläinen P J, *J Cardiovascular Pharmacology*, 26 (1995) 57.
- 7 Mebazaa B A, Nieminen M S, Packer M, Cohen-Solal A, Kleber F X, Pocock S J, Thakkar R, Padley R J, Pöder P & Kivikko M, *J Am Heart Assoc*, 297 (2007) 1883.
- 8 Archan S & Toller W, *Curr Opin Anaesthesiol*, 21 (2008) 78.
- 9 Asif M, *Current Med Chem*, 19 (2012) 2984.
- 10 Kumar D, Carron R, De La Calle C & Jinda D P, *Acta Pharm*, 58 (2008) 393.
- 11 Wang T, Dong Y, Wang L C & Chen Z, *Arzneimittelforschung*, 57 (2007) 641.
- 12 Jensen F, *Introduction to Computational Chemistry*, John Wiley and Sons Inc, New York, (1999).
- 13 Pulay P, *Mol Phys*, 17 (1969) 197.
- 14 Cook D B, *Ab-initio Valence Calculations in Chemistry*, John Wiley and Sons Inc, New York, 1974.
- 15 Gökce H & Bahçeli S, *J Mol Structr*, 1005 (1993) 100.
- 16 Frisch M J, et al, *Gaussian 09, Revision C 1*, Gaussian Inc, Wallingford, CT, (2009).
- 17 Dennington R, Keith T & Millam J, *GaussView, Version 5*, Semichem Inc, Shawnee Mission, KS, (2009).
- 18 Becke A D, *J Chem Phys*, 98 (1993) 5648.
- 19 Lee C, Yang W & Parr R G, *Phys Rev B*, 37 (1988) 785.
- 20 Foresman J B & Frisch E, *Exploring Chemistry with Electronic Structure Methods*. Gaussian Inc, Pittsburgh, PA, USA, 1993.
- 21 Gökce H & Bahçeli S, *Spectrochimica Acta A*, 96 (2012) 139.
- 22 Jamr Oz M H, *Vibrational Energy Distribution Analysis, VEDA4*, Warsaw, (2004).

- 23 Kereszture G, Holly S, Varga J, Besenyei G, Wang A Y & Durig J R, *Spectrochim Acta Part A*, 49 (1993) 2007.
- 24 Bellamy L J, *The Infrared Spectra of Complex Molecules*. Methuen&Co Ltd, London (1963).
- 25 Rui-Zhou Z & Xian-Zhou Z, *Indian J Pure & Appl Phys*, 51 (2013) 164.
- 26 Lambert J B, Shurvell H F & Cooks R G, *Introduction to Organic Spectroscopy*, New York, Macmillan Publishing, (1987).
- 27 Stuart B H, *Infrared Spectroscopy, Fundamentals & Applications*, England, John Willey & Sons, (2004).
- 28 Silverstein R M & Webster F X, *Spectroscopic Identification of Organic Compound*, New York: John Wiley & Sons, (1998).
- 29 Colthup N B, Lawrence H D & Wiberley S E, *Introduction to Infrared and Raman Spectroscopy*, New York: Academic Pres, 1964.
- 30 Süleymanoğlu N, Ustabas R, Alpaslan T B, Eydurhan F & İskeleli N O, *Spectrochimica Acta Part A*, 96 (2012) 35.
- 31 Fukui K, *Science*, 218 (1982) 747.
- 32 Pearson R G, *Proc Natl Acad Sci, U S A*, 83 (1986) 8440.
- 33 Szafran M, Komatsu A & Adamska E B, *J Mol Struct (THEOCHEM)*, 101 (2006) 827.
- 34 Muthu S & Paulraj E I, *J Chem Pharm Res*, 3(5), (2011) 323.
- 35 Pirnau A, Chiş V, Oniga O, Leopold N, Szabo L, Baias M & Cozar O, *Vib Spectrosc*, 289 (2008) 48.
- 36 Murray J S & Sen K, *Molecular Electrostatic Potentials Concepts and Applications*, Amsterdam, The Netherlands, Elsevier Science B V, (1996).
- 37 Smith P, *J Am Chem Soc*, 113 (1991) 6029.
- 38 Mulliken R S, *J Chem Phys*, 23 (1982) 1833.